1 **Sodium Thiosulfate, a source of Hydrogen Sulfide, stimulates endothelial cell proliferation and**
2 **neovascularization.**

3

4 Diane Macabrey[1], Jaroslava Joniová[2], Quentin Gasser[1], Clémence Bechelli[1], Alban Longchamp[1],
5 Severine Urfer[1], Martine Lambelet[1], Chun-Yu Fu[3], Guenter Schwarz[3], Georges Wagnieres[2], Sébastien
6 Déglise[1*] and Florent Allagnat[1*]

7 *[1]Department of Vascular Surgery, Lausanne University Hospital, Switzerland*

8 *[2]Laboratory for functional and metabolic imaging, LIFMET, Swiss Federal Institute of Technology (EPFL),*
9 *Lausanne, Switzerland.*

10 *[3]Institute of Biochemistry, Department of Chemistry, University of Cologne, Germany*

11 *These authors contributed equally to this work.

12

13

14 Corresponding Author:

15 Florent Allagnat

16 CHUV-Service de chirurgie vasculaire

17 Département des Sciences Biomédicales

18 Bugnon 7A, 1005 Lausanne, Suisse

19 Florent.allagnat@chuv.ch

20

21 Running title: sodium thiosulfate promotes angiogenesis

22

23 Word count: 7550

24 Six Figures

25 Category: original article

26

27 Keywords: angiogenesis; endothelial cells, proliferation; hydrogen sulfide; sodium thiosulfate,
28 arteriogenesis, endothelial cell metabolism, reperfusion, peripheral arterial disease.

29

30

31 **Abstract**

32

33 Therapies to accelerate vascular repair are currently lacking. Pre-clinical studies suggest that hydrogen
34 sulfide (H_2S), an endogenous gasotransmitter, promotes angiogenesis. Here, we hypothesized that
35 sodium thiosulfate (STS), a clinically relevant source of H_2S, would stimulate angiogenesis and vascular
36 repair.

37 STS stimulated neovascularization in WT and LDLR receptor knockout mice following hindlimb ischemia
38 as evidenced by increased leg perfusion assessed by laser Doppler imaging, and capillary density in the
39 gastrocnemius muscle. STS also promoted VEGF-dependent angiogenesis in matrigel plugs *in vivo* and
40 in the chorioallantoic membrane of chick embryos. *In vitro*, STS and NaHS stimulated HUVEC migration
41 and proliferation. Seahorse experiments further revealed that STS inhibited mitochondrial respiration
42 and promoted glycolysis in HUVECs. The effect of STS on migration and proliferation was glycolysis-
43 dependent.

44 STS probably acts through metabolic reprogramming of endothelial cells toward a more proliferative
45 glycolytic state. These findings may hold broad clinical implications for patients suffering from vascular
46 occlusive diseases.

47

48

Introduction

The prevalence of peripheral artery disease (PAD) is constantly rising as the prevalence of aging, hypertension, and diabetes mellitus[1, 2]. PAD is mostly due to atherosclerosis, which leads to progressive obstructions of peripheral arteries. When pharmacological therapy (lipid-lowering[3] and antihypertensive drugs[4]) and life-style changes (diet, exercise…[5]) fail and PAD progresses to critical limb threatening ischemia (CLTI), vascular surgery remains the only option[1, 2]. However, surgery may fail to relieve symptoms, or may not be possible due to the anatomy, severity of the disease or comorbidities. Thus, 20 to 40% of CLTI patients are not amenable to revascularization or have failed revascularization[6]. Even in the case of a successful surgery, residual microvascular disease may remain. New strategies to promote neovascularization and recovery following surgical revascularization in PAD and CLTI patients are required.

Hydrogen sulfide (H_2S) is a gasotransmitter produced in mammals via the reverse transsulfuration pathway[7]. H_2S is now recognized as having important vasorelaxant, cytoprotective and anti-inflammatory properties[7]. Moreover, pre-clinical *in vivo* studies showed that H_2S donors (NaHS, GYY4137) promote reperfusion in mice after femoral artery ligation in a model of hindlimb ischemia[8, 9]. Rushing et al. further showed that SG1002, a H_2S releasing pro-drug, increases leg neovascularization and collateral vessel formation after occlusion of the external iliac artery in miniswine[10]. In these studies, H_2S improved angiogenesis and arteriogenesis, two processes central for ischemic skeletal muscle repair[11, 12]. Overall, H_2S stimulates EC proliferation, migration and angiogenesis in a variety of pre-clinical models[13-15].

Mechanistically, H_2S stimulates the persulfidation of the VEGF receptor VEGFR2, promoting dimerization, auto phosphorylation and activation in EC[16]. H_2S also promotes eNOS activity and NO production, which is instrumental to angiogenesis[7]. In addition, H_2S inhibits mitochondrial oxidative phosphorylation, which in EC specifically, increases glycolytic ATP production to provide rapid energy for EC proliferation and migration[17]. However, despite these potent cardiovascular benefits in pre-clinical studies, H_2S-based therapeutics are not available yet.

Sodium thiosulfate ($Na_2S_2O_3$) is clinically-approved for the treatment of cyanide poisoning[18] and calciphylaxis, a rare condition of vascular calcification affecting patients with end-stage renal disease[19]. Sodium thiosulfate (STS) participates in sulfur metabolism within cells, releasing H_2S through non-enzymatic and enzymatic mechanisms[20, 21]. STS protects rat hearts from ischemia reperfusion injury[22], and we recently demonstrated that STS reduces intimal hyperplasia in pre-clinical models[23].

The aim of this study was to test whether STS stimulates arteriogenesis and angiogenesis in a mouse model of hindlimb ischemia (HLI). STS promoted vascular recovery following ischemia in WT and hypercholesterolemic LDLR$^{-/-}$ mice. STS also promoted VEGF-dependent angiogenesis *in vivo* in a matrigel plug assay and *in ovo* in the Chick Chorioallantoic Membrane (CAM) angiogenesis assay. As expected, STS promoted HUVEC proliferation and migration, similarly to other H_2S donors. Finally, STS inhibited mitochondrial respiration and promoted glycolysis in EC, and inhibition of glycolysis abrogated the effect of STS in HUVEC.

Material & Methods

1. Mice

WT mice C57BL/6JRj mice were purchased form Janvier Labs (Le Genest-Saint-Isle, France). LDLR$^{-/-}$ mice[24] (*Ldlr^{tm1Her}*, JAX stock #002207, kindly provided by Prof. Caroline Pot, Lausanne university

Hospital, Switzerland) were bred and housed in our animal facility and genotyped as previously described[24]. All mice were housed at standard housing conditions (22 °C, 12 h light/dark cycle), with ad libitum access to water and regular diet (SAFE®150 SP-25 vegetal diet, SAFE diets, Augy, France). LDLR$^{-/-}$ mice were put on a cholesterol rich diet (Western 1635, 0.2% Cholesterol, 21% Butter, U8958 Version 35, SAFE® Complete Care Competence) for 3 weeks prior to surgery. Mice were randomly treated with sodium thiosulfate (STS). Sodium Thiosulfate (Hänseler AG, Herisau, Switzerland) was given in mice water bottle at 2 or 4g/L to achieve 0.5 or 1 g/kg/day, changed 3 times a week.

Hindlimb ischemia surgery was performed under isoflurane anaesthesia (2.5% under 2.5 L O_2). Local anaesthesia was ensured by subcutaneous injection with a mix of lidocaine (6mg/kg) and bupivacaine (2.5mg/kg) along the incision line. The femoral artery was exposed through a small incision in the upper part of the leg. Two sutures (7-0 silk) were placed above the bifurcation with the epigastric artery. The femoral artery was then cut between the two sutures and the incision was closed with 5-0 prolene. Buprenorphine (0.1 mg/kg Temgesic, Reckitt Benckiser AG, Switzerland) was provided before surgery, as well as a post-operative analgesic every 12h for 36 hours. Perfusion of both operated and non-operated contralateral leg was monitored using a High Resolution Laser Doppler Imager (moorLDI2-HIR; Moor Instruments) under isoflurane anesthesia on a heating pad. Mice were euthanized under anaesthesia by cervical dislocation and exsanguination 2 weeks post-surgery. Muscles were either frozen in OCT for histology, or flash frozen directly in liquid nitrogen for molecular analyses.

Matrigel plug assay was conducted using Growth factor reduced Matrigel (BD Biosciences) supplemented with 20U/ml heparin (L6510, Seromed) and 200ng/ml human VEGF 165 (100-20, Peprotech), supplemented or not with 15mM STS. Under isoflurane anaesthesia (2.5% under 2.5 L O_2), 400-500µl of Matrigel was injected subcutaneously on the back of the mouse with a 25G needle. Matrigel plugs were isolated seven days after implantation, dissolved overnight in 0.1% Brij L23 (Sigma-Aldrich). Haemoglobin content was measured in a 96 well plate via colorimetric assay using 20µl of samples and 180 µl Drabkin's reagent (D5941, Sigma-Aldrich). Absorbance was measured after 20 min incubation at RT in the dark at 540nM using a Synergy Mx plate reader (BioTek Instruments AG, Switzerland). Data were plotted against a standard curve of ferrous stabilized human Haemoglobin A0 (H0267, Sigma-Aldrich).

EdU (A10044, ThermoFischer scientific) was diluted in NaCl at a concentration of 2mg/ml and 500 µg was injected via i.p. injection 16 hours before sacrifice. Mice were sacrificed at day 4 post HLI; ischemic muscles were placed in OCT and frozen in liquid nitrogen vapour.

All animal experimentations conformed to *the National Research Council:* Guide for the Care and Use of Laboratory Animals[25]. The Cantonal Veterinary Office (SCAV-EXPANIM, authorization number 3504) approved all animal care, surgery, and euthanasia procedures.

2. Cell culture
Pooled human umbilical vein endothelial cells (HUVECs; Lonza) were maintained in EGM™-2 (Endothelial Cell Growth Medium-2 BulletKit™; Lonza) at 37°C, 5% CO_2 and 5% O_2 as previously described[26]. Passages 1 to 8 were used for the experiments.

3. Chicken chorioallantoic membrane (CAM)
Fertilized brown chicken eggs were purchased from Animalco AG, Switzerland. Eggs were incubated for three days at 37 °C in a rotating incubator with the blunt end up. A small 3 mm diameter hole was made at embryo development day (EDD) 3. The Hole was covered with tape and the eggs placed back in the incubator in a stationary position. On EDD 11, the hole was enlarged to a diameter 25 mm, enabling topical administration of 20 µl of a fresh STS solution (500 µM – 20 mM in sodium chloride solution (NaCl; BioConcept, Switzerland)). On the control eggs, 20 µl of 0.9 % NaCl was added. The concentrations of STS are relative to the weight of the embryo at EDD 11. After STS administration, the hole was covered with a parafilm and eggs were returned to the incubator. At EDD 13, 20 µl of fluorescein isothiocyanate – dextran (25 kDa, 25 mg/ml; Sigma – Aldrich, Switzerland) dissolved in NaCl

was intravenously injected to the CAM's vascular network. At the same time, 100 µl of India ink (Parker) was injected under the CAM to improve the contrast between the blood vessels and extravascular space. It should be noted that India ink in this quantity and these conditions is not toxic to the CAM[27]. An epifluorescent microscope (Eclipse E 600 FN Nikon) was used for the acquisition of the angiograms using a 10x objective (Nikon, Plan Fluor, NA: 0.30, WD 16.0). Effect of STS on the vascular network of the CAM was quantified utilizing the quantitative analysis of the fluorescent angiograms in ImageJ Macro (NIH, Bethesda, Maryland) that was developed in our laboratory[28]. Five eggs were dedicated to one condition with three images taken per one egg (altogether, 15 images per condition were analysed).

4. Thiosulfate measurement

Urine and plasma were collected and stored in −80 °C until further analysis. Samples were kept on ice after thawing and centrifuged for 10 min at 15,000 rpm at 4 °C. 10 µL supernatant were mixed with 15 µL buffer (160 mM HEPES, and 16 mM EDTA, pH 8.0), 15 µL 100% acetonitrile, and 3 µL 46 mM monobromobimane (mBBr) and incubated for 30 min in the dark at 20 °C. Next 30 µL of 65 mM methanesulfonic acid was added as the stop solution and incubated again for 5 min in the dark at 20 °C before centrifugation for 15 min at 15,000 rpm and 4 °C. The supernatant was transferred to an HPLC vial and diluted 5-fold with running buffer A (0.25% acetic acid, pH 4.5). STS was analysed by HPLC on a C18 reversed-phase column (EC 250/3 NUCLEODUR C18 HTec, 5 µm, MACHEREY-NAGEL) at 40 °C and 0.9 mL/min in running buffer A. Against running buffer B (100% methanol) the following gradient profile was applied (Time [min]/Buffer B [%]): 0.00/15%, 0.75/15%, 2.65/23%, 5.43/33%, 6.03/37%, 8.06/45%, 8.44/65%, 8.82/100%, 11.34/100%, 11.72/15%, 15.00/15%. STS was detected by fluorescence using an excitation at 380 nm and emission at 480 nm and quantified by peak area integration in comparison to standard.

5. H_2S and persulfidation measurement

Free H_2S was measured in cells using the SF$_7$-AM fluorescent probe[29] (Sigma-Aldrich). The probe was dissolved in anhydrous DMF at 5 mM and used at 5 µM in serum-free EBM-2.

Global protein persulfidation was assessed on HUVEC grown on glass coverslips as previously described[23]. Cells were incubated for 20 minutes with 1mM 4-Chloro-7-nitrobenzofurazan (NBF-Cl, Sigma) diluted in PBS. Then, cells were washed with PBS and fixed for 10 minutes in ice-cold methanol. Coverslips were rehydrated in PBS, and incubated with 1mM NBF-Cl for 1h at 37°C. Cells were further incubated at 37°C for 1h in Daz2-Cy5.5 solution prepared as previously described[23]. Finally, coverslips were washed 3 times in methanol and 2 times in PBS, mounted in Vectashield mounting medium with DAPI, and visualized with a 90i Nikon fluorescence microscope.

6. Wound healing assay

HUVEC were grown to confluence in a 12-well plate and a scratch wound was created using a sterile p200 pipette tip. Repopulation of the wound in presence of Mitomycin C was recorded by phase-contrast microscopy over 16 hours in a Nikon Ti2-E live-cell microscope. The denuded area was measured at t=0h and t=10h after the wound using the ImageJ software. Data were expressed as a ratio of the healed area over the initial wound area.

6. BrdU assay

HUVEC were grown at 80% confluence (5.10^3 cells per well) on glass coverslips in a 24-well plate and starved overnight in serum-free medium (EBM-2, Lonza). Then, HUVEC were treated or not (ctrl) for 24 hours in full medium (EGM-2, Lonza) in presence of 10µM BrdU. All conditions were tested in parallel. Cells were fixed in ice-cold methanol 100 and immunostained for BrdU as previously described[23, 30, 31]. Images were acquired using a Nikon Eclipse 90i microscope. BrdU-positive nuclei and total DAPI-positive nuclei were automatically detected using the ImageJ software[26].

7. Seahorse

Glycolysis and Mitochondrial stress tests were performed on confluent HUVEC according to the manufacturer's kits and protocols (Agilent Seahorse XF glycolysis stress test kit, Agilent Technologies, Inc). 1µM Oligomycin was used. Data were analysed using the Seahorse Wave Desktop Software (Agilent Technologies, Inc. Seahorse Bioscience).

8. ATP Assay

HUVEC were grown at 80% confluence (10.10^3 cells per well) in a 12-well plate and starved overnight in serum-free medium (EBM-2, Lonza). Then, HUVEC were either treated or not (ctrl) with 3mM STS for 24 hours in full medium (EGM-2, Lonza), washed in ice-cold PBS and resuspended according to the ATP Assay Kit (Colorimetric/Fluorometric) (ab83355, Abcam).

9. Immunohistochemistry

Ischemic and contralateral gastrocnemius muscle were collected and flash frozen in OCT 2 weeks post-op. OCT blocks were cut into 10 µM slides for immunostaining. Muscle sections were permeabilised in PBS supplemented with 2 wt. % BSA and 0.1 vol. % Triton X-100 for 30 min, blocked in PBS supplemented with 2 wt. % BSA and 0.1 vol. % Tween 20 for another 30 min, and incubated overnight using the antibodies described in **Supplemental Table 1** diluted in the same buffer. The slides were then washed 3 times for 5 min in PBS supplemented with 0.1 vol. % Tween 20, and incubated for 1 h at room temperature with a mix of appropriate fluorescent-labelled secondary antibodies. Muscle fibre type staining were performed using the antibody developed by Sciaffino[32]. EdU immunostaining was performed according to the manufacturer's instructions (Click-iT™ Plus EdU Cell Proliferation Kit for Imaging, Alexa Fluor™ 594 dye, ThermoFischer). Images were acquired using a ZEISS Axioscan 7 Microscope Slide Scanner.

10. Reverse transcription and quantitative polymerase chain reaction (RT-qPCR)

HUVEC or grinded frozen gastrocnemius muscles were homogenised in Tripure Isolation Reagent (Roche, Switzerland), and total RNA was extracted according to the manufacturer's instructions. After RNA Reverse transcription (Prime Script RT reagent, Takara), cDNA levels were measured by qPCR Fast SYBR™ Green Master Mix (Ref: 4385618, Applied Biosystems, ThermoFischer Scientific AG, Switzerland) in a Quant Studio 5 Real-Time PCR System (Applied Biosystems, ThermoFischer Scientific AG, Switzerland), using the primers given in the **Supplemental Table 2**.

11. Statistical analyses

All experiments adhered to the ARRIVE guidelines and followed strict randomization. All experiments and data analysis were conducted in a blind manner using coded tags rather than actual group name. A power analysis was performed prior to the study to estimate sample-size. We hypothesized that STS would improve neovascularization by 20%. Using an SD at +/- 10% for the surgery and considering a power at 0.8, we calculated that n= 8 animals/group was necessary to validate a significant effect of the STS. Animals with pre-existing conditions (malocclusion, injury, abnormal weight) were not operated or excluded from the experiments upon discovery during dissection. All experiments were analysed using GraphPad Prism 9. Normal distribution of the data was assessed using Kolmogorov-Smirnov tests. All data had a normal distribution. Unpaired bilateral Student's t-tests, or one or two-ways ANOVA were performed followed by multiple comparisons using post-hoc t-tests with the appropriate correction for multiple comparisons.

Results

   1. STS promotes reperfusion and muscle recovery in a mouse model of hindlimb ischemia

To test the benefits of STS on vascular recovery, hindlimb ischemia (HLI) was induced by transection of the femoral artery, which leads to ischemia-induced muscle damage. Laser Doppler imaging showed that HLI reduced blood flow by >80% both in Ctrl and mice treated with 2 or 4g/L of STS. Doppler imaging further revealed that 2g/L STS improved reperfusion (**Figure 1A**), while 4g/L tended to increase blood flow compared to Ctrl mice (**Figure 1C**). Morphological analysis of the gastrocnemius muscle 14 days post-surgery further showed that STS reduced muscle damaged as assessed by the mean muscle fibre cross-sectional area (**Figure 1B, D).** We also performed the HLI on hypercholesterolemic LDLR$^{-/-}$ mice fed for 3 weeks with a cholesterol-rich diet, a model closer to the dyslipidaemia state of PAD patients. 2g/L STS also increased reperfusion (**Figure 1E**) and reduced muscle damage (**Figure 1F)** in this diseased model.

   2. STS leads to enzymatic production of H$_2$S and increases protein persulfidation

We previously demonstrated that STS behaves as a H$_2$S donor[23, 33]. To test whether STS releases detectable amounts of H$_2$S in HUVECs, we used the H$_2$S specific probe SF$_7$-AM [29]. SF$_7$-AM signal was monitored in HUVECs 90 min post addition of 15mM STS, and showed a 50% increase in SF$_7$-AM signal (**Figure 2A**). In vivo, STS treatment via the water bottle at 4g/L significantly increased circulating levels of thiosulfate (**Figure 2B**) and urinary excretion of mM amounts of thiosulfate (**Figure 2C**). Thiosulfate is an intermediate of sulfur metabolism metabolized by the H$_2$S biosynthetic pathway and sulfide-oxidizing unit[34, 35]. A 4h treatment with STS, but not NaHS, increased the mRNA expression of sulfite oxidase (SUOX), thiosulfate sulfurtransferase-like domain containing 1 (TSTD1), mercaptopyruvate sulfurtransferase (MPST), but not thiosulfate sulfurtransferase (TST) in HUVECs (**Figure 2D**). However, neither STS nor NaHS influenced the mRNA expression of H$_2$S-generating enzymes CBS and CSE (**Figure S1**). Of note, both NaHS and STS increased the expression of the mitochondrial H$_2$S-detoxifing enzymes sulfide quinone oxidoreductase (SQOR) and persulfide dioxygenase ETHE1 (**Figure 2D).** In gastrocnemius muscles from mice treated with 4g STS for 1 week, STS treatment increased mRNA expression of Tstd2 and Sqor, whereas the expression of Tst was decreased. STS did not affect the mRNA expression of Suox, Mpst and Ethe1 (**Figure 2E**). H$_2$S signals through post-translational modifications of reactive cysteine residues by persulfidation[36, 37]. Both STS and NaHS increased protein persulfidation as measured by DAZ-2-Cy5.5 labelling of persulfide residues in HUVEC treated for 4 hours with 100 μM NaHS or 15mM STS **(Figure 2F).**

   3. STS promotes arteriogenesis and angiogenesis in vivo

To test whether STS increased blood perfusion via improved micro-vessel regeneration, we determined the micro-vessel density in the gastrocnemius muscle using VE-Cadherin immunofluorescent staining of WT mice. Both 2 and 4g/L STS treatment increased the micro-vessel density as compared to Ctrl mice 14 days after HLI **(Figure 3A-B)**. STS treatment also increased the micro-vessel density in LDLR$^{-/-}$ mice **(Figure 3C)**. EdU/Erg immunofluorescent staining on ischemic muscles 4 days after ischemia showed that STS increased the percentage of EC (**Figure 3D, E**) and proliferating EC in WT mice (**Figure 3D, F**). Then, we assessed the effect of STS on angiogenesis *in ovo* using the Chicken chorioallantoic membrane (CAM) assay and the Matrigel plug assay. STS was applied topically to achieve 0.5 or 5mM at embryonic development day 11 (EDD11). Observations at EDD13 revealed that STS promoted the capillary formation measured as the relative number of branching points/mm^2, relative mean mesh size and Q3 mesh area of the vessel network (**Figure 3G**). The addition of 15mM STS in Matrigel plugs also promoted VEGF-induced angiogenesis as assessed by haemoglobin

content 7 days after subcutaneous injection in the mouse (**Figure 3H**). To investigate the effect of STS on EC directly, we assessed the proliferation and migration of primary human umbilical vein endothelial cells (HUVECs). STS increased HUVEC proliferation (**Figure 3I**), similarly to the H_2S donor salt NaHS and the slow-releasing H_2S donor GYY4137 (**Figure S2**). STS also promoted HUVEC migration in a wound healing assay (**Figure 3J**). To further study endothelial function, we investigated known markers of endothelial function[38]. A 4h treatment with 3mM STS increased eNOS and VEGFR2 mRNA expression in HUVEC (**Figure S3A).** Western blot analysis from mice who underwent hindlimb ischemia treated with STS for 2 weeks revealed that 2 g/L STS increased the ratio of P-eNOS over eNOS and increased the ratio of P-VEGFR2/VEGFR2 levels in the ischemic gastrocnemius muscle (**Figure S3B**). Of note, this chronic long-term treatment decreased total eNOS and VEGFR2 protein levels.

4. STS limits inflammation and muscle damage 4 days after ischemia

After ischemia, inflammation plays a major role in muscle function and repair. Specifically, macrophages shifted toward the M2 phenotype are instrumental in arteriogenesis following ischemia[39]. STS limited muscle damage in the gastrocnemius muscle of mice 4 days after HLI, as assessed by laminin staining (**Figure 4A**). Of note, there is no correlation between muscle damage and percentage of ischemia at day 0 (**Figure 4A**). Decreased muscle damage was accompanied by a significant reduction in macrophage infiltration, as assessed by CD68$^+$ staining. Furthermore, STS increased the percentage of HO1$^+$ CD68$^+$ macrophages, a marker of M2 pro-resolving macrophages (**Figure 4B**). Given that STS improves muscle repair, we further studied muscle fibre type distribution pre and 14 days post-op in mice treated or not with STS (**Figure S4**). Pre-op immunostaining of type I, type IIA and type IIB fibres showed that the soleus was composed of 60% type I slow (I, Myh7 in blue) and 40% of fast (IIA, Myh2 in red) oxidative fibres. The gastrocnemius was made of more than 80% of fast glycolytic IIB fibres (type IIB, Myh4 in green), and 10% of type IIA located toward the soleus. The remaining were mainly negative fibres. Type I fibres constituted less than 1 % of the total fibres in the gastrocnemius. Post-ischemia in the soleus, which suffered the most from ischemic injury, hybrid type I/IIA fibres (red blue = purple) almost completely replaced type I fibres. In the gastrocnemius, IIB fibres were significantly reduced, while type IIA increased to 15% and hybrid type I/IIA fibres appear. STS increased the proportion of hybrid type I/IIA fibres in both muscles (**Figure S4).**

5. STS inhibits mitochondrial respiration and increases glycolysis and ATP production in HUVECs

ECs are glycolytic, thus favouring glycolysis for ATP production. This key feature allows EC to proliferate and migrate in hypoxic conditions in the context of angiogenesis[40, 41]. H_2S blocks mitochondrial respiration through inhibition of the complex IV of the mitochondria, which increases compensatory glycolysis in EC and promotes angiogenesis[17]. To test the effect of STS on mitochondrial respiration, we performed a mitochondrial stress test in a seahorse apparatus. 3mM STS rapidly reduced oxygen consumption rate (OCR) in HUVEC **(Figure 5A).** A 4-hour pre-treatment with STS dose-dependently inhibited mitochondrial respiration in HUVEC, leading to reduced basal and max respiration and ATP production in that assay **(Figure 5B).** To measure the cell's glycolytic reserve, i.e. the ability to increase glycolysis upon inhibition of respiration, we then performed a glycolysis stress test on HUVEC pre-treated for 4 hours with STS or NaHS. Inhibition of mitochondrial respiration using oligomycin promoted glycolysis in HUVEC. The donors increased basal glycolysis in HUVEC, thereby reducing the glycolytic reserve **(Figure 5B).** We further confirmed that an 8-hour treatment with 3mM STS increased ATP production in HUVECs **(Figure 5C).** In EC, the enzyme PFKFB3 tightly regulates glycolysis[39]. A 4-hour pre-treatment with 15mM STS stimulated mRNA expression of key glycolysis genes in HUVEC. In

315 the gastrocnemius, one week treatment with 4g/L of STS significantly increased the mRNA expression
316 of PFKFB3, whereas the mRNA of PKM was not affected (**Figure 5D**).

317   *6.   STS-induced HUVEC proliferation requires glycolysis*
318 To confirm that the effect of STS on angiogenesis is glycolysis-dependent, we assessed the proliferation
319 of HUVECs, in presence or not of the glycolysis inhibitor 3PO or the glucose competitor 2-deoxy-glucose
320 (2-DG). Both 3PO **(Figure 6A)** and 2-DG **(Figure 6B)** treatment reduced basal HUVEC proliferation and
321 fully abolished the positive effect of STS on proliferation**.**

322

323

Discussion

Despite potent cardiovascular benefits, there is no clinically approved H_2S-releasing molecule. STS does not directly release H_2S, but provide thiosulfate, which can further lead to formation of H_2S and polysulfides via rhodanese activity and the reverse transsulfuration pathway[20]. Our study demonstrate that STS treatment promotes the enzymatic metabolism of thiosulfate through both the H_2S biosynthetic pathway and sulfide oxidizing unit[34, 35], yielding minutes amounts of H_2S with measurable effects on global protein persulfidation. The fact that STS increased protein persulfidation suggests that STS works similarly as a H_2S donor[42]. This is in line with previous studies showing that thiosulfate can be metabolized to H_2S through sulfite formation or bound sulfane sulfur release[20, 33, 43-45].

In line with previous studies using other sources of H_2S[8-10], STS increases revascularization *in vivo* following hindlimb ischemia. Reminiscent of other studies performed with NaHS[13, 46, 47], STS also promotes angiogenesis in the CAM model and specifically promotes VEGF-driven sprouting angiogenesis in matrigel plug implants. At the cellular levels, STS stimulates EC proliferation and migration *in vitro* in cultured endothelial cells, and *in vivo* in the ischemic muscle, leading to increased capillary density and blow flow.

The fact that STS promoted VEGF-dependent sprouting angiogenesis in matrigel plugs, but also neovascularization in the HLI model, suggest that STS/H_2S may act on different levels to promote neovascularization. First, H_2S is known to promote angiogenesis via stimulation of the VEGFR2 and NO pathway[16, 48-50]. In this study, we also oberved that STS stimulates the VEGFR2 and eNOS pathways *in vitro* and *in vivo* in the muscle post HLI. Second, we previously showed that H_2S promotes the metabolic switch in EC to favour glycolysis, and this mechanism promotes VEGF-induced EC migration[17]. Indeed, EC rely mostly on glycolysis for energy production and further upregulate glycolysis to fuel migration and proliferation during angiogenesis[40, 41]. Here, STS inhibited mitochondrial respiration, inducing a compensatory increase in glycolysis, which seems instrumental to observe STS-induced EC proliferation. *In vivo* data also suggest that STS treatment modulates the expression of genes involved in glycolysis. Third and last, neovascularization in the HLI model is mediated by both arteriogenesis and angiogenesis. Arteriogenesis is driven by shear stress and requires macrophages to achieve proper vessel remodeling[51, 52]. In particular, pro-resolving macrophages shifted toward the M2 phenotype are instrumental for arteriogenesis following skeletal ischemia[53]. In line with a role of macrophages in early recovery and arteriogenesis, we observed massive macrophage infiltration in the muscle 4 days after HLI. Our data indicate an anti-inflammatory effect of STS, and suggest a shift toward HO-1^{+} pro-repair M2 macrophages[54]. Interestingly, H_2S possesses anti-inflammatory properties[55] and was suggested to promote the shift toward the M2 phenotype in the context of atherosclerosis[56]. Given that the increase in HO1^{+}macrophages is accompanied by a decrease in total macrophages, the exact impact of STS on macrophage polarization remains to be clarify to determine whether STS inhibits inflammation in general, or specifically promotes the M2 phenotype. Reduced inflammation could a bystander effect of accelerated neovascularization. Further studies remain to be performed to test the respective role of metabolic reprogramming, VEGF potentiation and anti-inflammatory properties of STS to improve recovery in the HLI model. Overall, we propose that STS acts at several levels to promote both arteriogenesis and angiogenesis.

To replicate some of the comorbidities of PAD patients, we further confirmed that STS improved neovascularization in hypercholesterolemic mice. However, the HLI model remains a model of acute

366 ischemia, with limited impairment in limb function and fast reperfusion to asymptomatic levels, even
367 in hypercholesterolemic mice. In addition, further studies are required to assess the function and
368 leakiness of neovessels in response to STS.

369 STS is clinically approved and safe in gram quantities in humans. We recently showed that oral STS at
370 4g/L has no toxicity on mice[23]. Here, we show that STS at 4g/L leads to a modest increase in circulating
371 thiosulfate levels, while most of the thiosulfate absorbed in probably eliminated in the urine.
372 Additional experiments are required to assess STS accumulation and distribution in tissues. The fact
373 that STS was more potent in stimulating revascularization at 2g/L than at 4g/L suggest a narrow
374 therapeutic range for the pro-angiogenic effects of STS.

375 In conclusion, STS, a molecule with high translational potential since already approved clinically,
376 promotes EC proliferation and recovery after hindlimb ischemia, both in WT and hypercholesterolemic
377 LDLR$^{-/-}$ mice. STS promotes EC proliferation in a glycolysis-dependent manner. We recently showed
378 that STS inhibits intimal hyperplasia, which is the bane of all surgical revascularization[23]. These findings
379 suggest that STS holds strong potential to promote vascular repair in PAD patients, while limiting
380 intimal hyperplasia. Altogether, this calls for further pre-clinical studies in the large animal, and
381 prospective clinical trials in patients.

382

395

396 **Author Contribution Statement**.
397 FA, AL and SD designed the study. FA, JJ, QG, DM, C-Y F and ML performed the experiments. FA, JJ, DM
398 and ML, GS, GW and SD analyzed the data. FA, DM, AL and SD wrote the manuscript. All Authors
399 critically revised the manuscript. FA and DM finalized the manuscript.

400

401 **Conflict of Interest:** none declared.

402

403 **References**

404   1.   Eraso LH, Fukaya E, Mohler ER, 3rd, Xie D, Sha D, Berger JS. Peripheral arterial disease,
405 prevalence and cumulative risk factor profile analysis. European journal of preventive
406 cardiology. 2014;21(6):704-11. DOI: 10.1177/2047487312452968.

407   2.   Song P, Rudan D, Zhu Y, Fowkes FJI, Rahimi K, Fowkes FGR, Rudan I. Global, regional,
408 and national prevalence and risk factors for peripheral artery disease in 2015: an updated
409 systematic review and analysis. Lancet Glob Health. 2019;7(8):e1020-e30. DOI:
410 10.1016/S2214-109X(19)30255-4.

411   3.   Arao K, Yasu T, Endo Y, Funazaki T, Ota Y, Shimada K, Tokutake E, Naito N, Takase B,
412 Wake M, Ikeda N, Horie Y, Sugimura H, Momomura SI, Kawakami M, Investigators of the A-A,
413 Lipid Lowering with Pitavastatin Evaluation Study in N. Effects of pitavastatin on walking
414 capacity and CD34(+)/133(+) cell number in patients with peripheral artery disease. Heart
415 Vessels. 2017;32(10):1186-94. DOI: 10.1007/s00380-017-0988-1.

416   4.   Shahin Y, Barnes R, Barakat H, Chetter IC. Meta-analysis of angiotensin converting
417 enzyme inhibitors effect on walking ability and ankle brachial pressure index in patients with
418 intermittent claudication. Atherosclerosis. 2013;231(2):283-90. DOI:
419 10.1016/j.atherosclerosis.2013.09.037.

420   5.   Lane R, Ellis B, Watson L, Leng GC. Exercise for intermittent claudication. Cochrane
421 Database Syst Rev. 2014(7):CD000990. DOI: 10.1002/14651858.CD000990.pub3.

422   6.   Iyer SR, Annex BH. Therapeutic Angiogenesis for Peripheral Artery Disease: Lessons
423 Learned in Translational Science. JACC Basic Transl Sci. 2017;2(5):503-12. DOI:
424 10.1016/j.jacbts.2017.07.012.

425   7.   Cirino G, Szabo C, Papapetropoulos A. Physiological roles of hydrogen sulfide in
426 mammalian cells, tissues and organs. Physiol Rev. 2022. DOI: 10.1152/physrev.00028.2021.

427   8.   Majumder A, Singh M, George AK, Behera J, Tyagi N, Tyagi SC. Hydrogen sulfide
428 improves postischemic neoangiogenesis in the hind limb of cystathionine-beta-synthase
429 mutant mice via PPAR-gamma/VEGF axis. Physiol Rep. 2018;6(17):e13858. DOI:
430 10.14814/phy2.13858.

431   9.   Wang MJ, Cai WJ, Li N, Ding YJ, Chen Y, Zhu YC. The hydrogen sulfide donor NaHS
432 promotes angiogenesis in a rat model of hind limb ischemia. Antioxid Redox Signal.
433 2010;12(9):1065-77. DOI: 10.1089/ars.2009.2945.

434   10.   Rushing AM, Donnarumma E, Polhemus DJ, Au KR, Victoria SE, Schumacher JD, Li Z,
435 Jenkins JS, Lefer DJ, Goodchild TT. Effects of a novel hydrogen sulfide prodrug in a porcine
436 model of acute limb ischemia. J Vasc Surg. 2019;69(6):1924-35. DOI:
437 10.1016/j.jvs.2018.08.172.

438   11.   Annex BH, Cooke JP. New Directions in Therapeutic Angiogenesis and Arteriogenesis
439 in Peripheral Arterial Disease. Circ Res. 2021;128(12):1944-57. DOI:
440 10.1161/CIRCRESAHA.121.318266.

441   12.   Yuan S, Kevil CG. Nitric Oxide and Hydrogen Sulfide Regulation of Ischemic Vascular
442 Remodeling. Microcirculation. 2016;23(2):134-45. DOI: 10.1111/micc.12248.

443   13.   Papapetropoulos A, Pyriochou A, Altaany Z, Yang G, Marazioti A, Zhou Z, Jeschke MG,
444 Branski LK, Herndon DN, Wang R, Szabo C. Hydrogen sulfide is an endogenous stimulator of
445 angiogenesis. Proc Natl Acad Sci U S A. 2009;106(51):21972-7. DOI:
446 10.1073/pnas.0908047106.

447   14.   Polhemus DJ, Kondo K, Bhushan S, Bir SC, Kevil CG, Murohara T, Lefer DJ, Calvert JW.
448 Hydrogen sulfide attenuates cardiac dysfunction after heart failure via induction of
449 angiogenesis. Circ Heart Fail. 2013;6(5):1077-86. DOI:
450 10.1161/CIRCHEARTFAILURE.113.000299.

451 15.   Jang H, Oh MY, Kim YJ, Choi IY, Yang HS, Ryu WS, Lee SH, Yoon BW. Hydrogen sulfide
452 treatment induces angiogenesis after cerebral ischemia. J Neurosci Res. 2014;92(11):1520-8.
453 DOI: 10.1002/jnr.23427.

454 16.   Tao BB, Liu SY, Zhang CC, Fu W, Cai WJ, Wang Y, Shen Q, Wang MJ, Chen Y, Zhang LJ,
455 Zhu YZ, Zhu YC. VEGFR2 functions as an H2S-targeting receptor protein kinase with its novel
456 Cys1045-Cys1024 disulfide bond serving as a specific molecular switch for hydrogen sulfide
457 actions in vascular endothelial cells. Antioxid Redox Signal. 2013;19(5):448-64. DOI:
458 10.1089/ars.2012.4565.

459 17.   Longchamp A, Mirabella T, Arduini A, MacArthur MR, Das A, Trevino-Villarreal JH, Hine
460 C, Ben-Sahra I, Knudsen NH, Brace LE, Reynolds J, Mejia P, Tao M, Sharma G, Wang R,
461 Corpataux JM, Haefliger JA, Ahn KH, Lee CH, Manning BD, Sinclair DA, Chen CS, Ozaki CK,
462 Mitchell JR. Amino Acid Restriction Triggers Angiogenesis via GCN2/ATF4 Regulation of VEGF
463 and H2S Production. Cell. 2018;173(1):117-29 e14. DOI: 10.1016/j.cell.2018.03.001.

464 18.   Bebarta VS, Brittain M, Chan A, Garrett N, Yoon D, Burney T, Mukai D, Babin M, Pilz RB,
465 Mahon SB, Brenner M, Boss GR. Sodium Nitrite and Sodium Thiosulfate Are Effective Against
466 Acute Cyanide Poisoning When Administered by Intramuscular Injection. Ann Emerg Med.
467 2017;69(6):718-25 e4. DOI: 10.1016/j.annemergmed.2016.09.034.

468 19.   Nigwekar SU, Thadhani R, Brandenburg VM. Calciphylaxis. N Engl J Med.
469 2018;378(18):1704-14. DOI: 10.1056/NEJMra1505292.

470 20.   Olson KR, Deleon ER, Gao Y, Hurley K, Sadauskas V, Batz C, Stoy GF. Thiosulfate: a
471 readily accessible source of hydrogen sulfide in oxygen sensing. Am J Physiol Regul Integr
472 Comp Physiol. 2013;305(6):R592-603. DOI: 10.1152/ajpregu.00421.2012.

473 21.   Snijder PM, Frenay AR, de Boer RA, Pasch A, Hillebrands JL, Leuvenink HG, van Goor H.
474 Exogenous administration of thiosulfate, a donor of hydrogen sulfide, attenuates angiotensin
475 II-induced hypertensive heart disease in rats. Br J Pharmacol. 2015;172(6):1494-504. DOI:
476 10.1111/bph.12825.

477 22.   Ravindran S, Kurian GA. Effect of Sodium Thiosulfate Postconditioning on Ischemia-
478 Reperfusion Injury Induced Mitochondrial Dysfunction in Rat Heart. J Cardiovasc Transl Res.
479 2018;11(3):246-58. DOI: 10.1007/s12265-018-9808-y.

480 23.   Macabrey D, Longchamp A, MacArthur MR, Lambelet M, Urfer S, Deglise S, Allagnat F.
481 Sodium thiosulfate acts as a hydrogen sulfide mimetic to prevent intimal hyperplasia via
482 inhibition of tubulin polymerisation. EBioMedicine. 2022;78:103954. DOI:
483 10.1016/j.ebiom.2022.103954.

484 24.   Ishibashi S, Brown MS, Goldstein JL, Gerard RD, Hammer RE, Herz J.
485 Hypercholesterolemia in low density lipoprotein receptor knockout mice and its reversal by
486 adenovirus-mediated gene delivery. J Clin Invest. 1993;92(2):883-93. DOI: 10.1172/JCI116663.

487 25.   National Research Council (U.S.). Committee for the Update of the Guide for the Care
488 and Use of Laboratory Animals., Institute for Laboratory Animal Research (U.S.), National
489 Academies Press (U.S.). Guide for the care and use of laboratory animals. 8th ed. Washington,
490 D.C.: National Academies Press; 2011. xxv, 220 p. p.

491 26.   Longchamp A, Kaur K, Macabrey D, Dubuis C, Corpataux JM, Deglise S, Matson JB,
492 Allagnat F. Hydrogen sulfide-releasing peptide hydrogel limits the development of intimal
493 hyperplasia in human vein segments. Acta Biomater. 2019. DOI:
494 10.1016/j.actbio.2019.07.042.

495 27.   Joniova J, Wagnieres G. Catechin reduces phototoxic effects induced by
496 protoporphyrin IX-based photodynamic therapy in the chick embryo chorioallantoic
497 membrane. J Biomed Opt. 2020;25(6):1-9. DOI: 10.1117/1.JBO.25.6.063807.

28.   Nowak-Sliwinska P, Ballini JP, Wagnieres G, van den Bergh H. Processing of fluorescence angiograms for the quantification of vascular effects induced by anti-angiogenic agents in the CAM model. Microvasc Res. 2010;79(1):21-8. DOI: 10.1016/j.mvr.2009.10.004.

29.   Lin VS, Lippert AR, Chang CJ. Cell-trappable fluorescent probes for endogenous hydrogen sulfide signaling and imaging H_2O_2-dependent H_2S production. Proc Natl Acad Sci U S A. 2013;110(18):7131-5. DOI: 10.1073/pnas.1302193110.

30.   Macabrey D, Deslarzes-Dubuis C, Longchamp A, Lambelet M, Ozaki CK, Corpataux JM, Allagnat F, Deglise S. Hydrogen Sulphide Release via the Angiotensin Converting Enzyme Inhibitor Zofenopril Prevents Intimal Hyperplasia in Human Vein Segments and in a Mouse Model of Carotid Artery Stenosis. Eur J Vasc Endovasc Surg. 2022;63(2):336-46. DOI: 10.1016/j.ejvs.2021.09.032.

31.   Longchamp A, Kaur K, Macabrey D, Dubuis C, Corpataux JM, Deglise S, Matson JB, Allagnat F. Hydrogen sulfide-releasing peptide hydrogel limits the development of intimal hyperplasia in human vein segments. Acta Biomater. 2019;97:374-84. DOI: 10.1016/j.actbio.2019.07.042.

32.   Schiaffino S, Gorza L, Sartore S, Saggin L, Ausoni S, Vianello M, Gundersen K, Lomo T. Three myosin heavy chain isoforms in type 2 skeletal muscle fibres. J Muscle Res Cell Motil. 1989;10(3):197-205. DOI: 10.1007/BF01739810.

33.   Macabrey D, Longchamp A, MacArthur MR, Lambelet M, Urfer S, Corpataux J-M, Deglise S, Allagnat F. Sodium Thiosulfate acts as an H_2S mimetic to prevent intimal hyperplasia via inhibition of tubulin polymerization. bioRxiv. 2021.

34.   Paul BD, Snyder SH, Kashfi K. Effects of hydrogen sulfide on mitochondrial function and cellular bioenergetics. Redox Biol. 2021;38:101772. DOI: 10.1016/j.redox.2020.101772.

35.   Olson KR. H2S and polysulfide metabolism: Conventional and unconventional pathways. Biochem Pharmacol. 2018;149:77-90. DOI: 10.1016/j.bcp.2017.12.010.

36.   Li Z, Polhemus DJ, Lefer DJ. Evolution of Hydrogen Sulfide Therapeutics to Treat Cardiovascular Disease. Circ Res. 2018;123(5):590-600. DOI: 10.1161/CIRCRESAHA.118.311134.

37.   Zivanovic J, Kouroussis E, Kohl JB, Adhikari B, Bursac B, Schott-Roux S, Petrovic D, Miljkovic JL, Thomas-Lopez D, Jung Y, Miler M, Mitchell S, Milosevic V, Gomes JE, Benhar M, Gonzalez-Zorn B, Ivanovic-Burmazovic I, Torregrossa R, Mitchell JR, Whiteman M, Schwarz G, Snyder SH, Paul BD, Carroll KS, Filipovic MR. Selective Persulfide Detection Reveals Evolutionarily Conserved Antiaging Effects of S-Sulfhydration. Cell Metab. 2019;30(6):1152-70 e13. DOI: 10.1016/j.cmet.2019.10.007.

38.   Heiss C, Rodriguez-Mateos A, Kelm M. Central role of eNOS in the maintenance of endothelial homeostasis. Antioxid Redox Signal. 2015;22(14):1230-42. DOI: 10.1089/ars.2014.6158.

39.   De Bock K, Georgiadou M, Schoors S, Kuchnio A, Wong BW, Cantelmo AR, Quaegebeur A, Ghesquiere B, Cauwenberghs S, Eelen G, Phng LK, Betz I, Tembuyser B, Brepoels K, Welti J, Geudens I, Segura I, Cruys B, Bifari F, Decimo I, Blanco R, Wyns S, Vangindertael J, Rocha S, Collins RT, Munck S, Daelemans D, Imamura H, Devlieger R, Rider M, Van Veldhoven PP, Schuit F, Bartrons R, Hofkens J, Fraisl P, Telang S, Deberardinis RJ, Schoonjans L, Vinckier S, Chesney J, Gerhardt H, Dewerchin M, Carmeliet P. Role of PFKFB3-driven glycolysis in vessel sprouting. Cell. 2013;154(3):651-63. DOI: 10.1016/j.cell.2013.06.037.

40.   Zecchin A, Kalucka J, Dubois C, Carmeliet P. How Endothelial Cells Adapt Their Metabolism to Form Vessels in Tumors. Front Immunol. 2017;8:1750. DOI: 10.3389/fimmu.2017.01750.

545 41. Eelen G, de Zeeuw P, Treps L, Harjes U, Wong BW, Carmeliet P. Endothelial Cell
546 Metabolism. Physiol Rev. 2018;98(1):3-58. DOI: 10.1152/physrev.00001.2017.
547 42. Fu L, Liu K, He J, Tian C, Yu X, Yang J. Direct Proteomic Mapping of Cysteine
548 Persulfidation. Antioxid Redox Signal. 2019. DOI: 10.1089/ars.2019.7777.
549 43. Marutani E, Yamada M, Ida T, Tokuda K, Ikeda K, Kai S, Shirozu K, Hayashida K, Kosugi
550 S, Hanaoka K, Kaneki M, Akaike T, Ichinose F. Thiosulfate Mediates Cytoprotective Effects of
551 Hydrogen Sulfide Against Neuronal Ischemia. J Am Heart Assoc. 2015;4(11). DOI:
552 10.1161/JAHA.115.002125.
553 44. Lee M, McGeer EG, McGeer PL. Sodium thiosulfate attenuates glial-mediated
554 neuroinflammation in degenerative neurological diseases. J Neuroinflammation. 2016;13:32.
555 DOI: 10.1186/s12974-016-0488-8.
556 45. Kolluru GK, Shen X, Bir SC, Kevil CG. Hydrogen sulfide chemical biology:
557 pathophysiological roles and detection. Nitric Oxide. 2013;35:5-20. DOI:
558 10.1016/j.niox.2013.07.002.
559 46. Katsouda A, Bibli SI, Pyriochou A, Szabo C, Papapetropoulos A. Regulation and role of
560 endogenously produced hydrogen sulfide in angiogenesis. Pharmacol Res. 2016;113(Pt
561 A):175-85. DOI: 10.1016/j.phrs.2016.08.026.
562 47. Cai WJ, Wang MJ, Moore PK, Jin HM, Yao T, Zhu YC. The novel proangiogenic effect of
563 hydrogen sulfide is dependent on Akt phosphorylation. Cardiovasc Res. 2007;76(1):29-40.
564 DOI: 10.1016/j.cardiores.2007.05.026.
565 48. Kolluru GK, Bir SC, Yuan S, Shen X, Pardue S, Wang R, Kevil CG. Cystathionine gamma-
566 lyase regulates arteriogenesis through NO-dependent monocyte recruitment. Cardiovasc Res.
567 2015;107(4):590-600. DOI: 10.1093/cvr/cvv198.
568 49. Potenza DM, Guerra G, Avanzato D, Poletto V, Pareek S, Guido D, Gallanti A, Rosti V,
569 Munaron L, Tanzi F, Moccia F. Hydrogen sulphide triggers VEGF-induced intracellular Ca(2)(+)
570 signals in human endothelial cells but not in their immature progenitors. Cell Calcium.
571 2014;56(3):225-34. DOI: 10.1016/j.ceca.2014.07.010.
572 50. Bir SC, Kolluru GK, McCarthy P, Shen X, Pardue S, Pattillo CB, Kevil CG. Hydrogen sulfide
573 stimulates ischemic vascular remodeling through nitric oxide synthase and nitrite reduction
574 activity regulating hypoxia-inducible factor-1alpha and vascular endothelial growth factor-
575 dependent angiogenesis. J Am Heart Assoc. 2012;1(5):e004093. DOI:
576 10.1161/JAHA.112.004093.
577 51. Fung E, Helisch A. Macrophages in collateral arteriogenesis. Front Physiol. 2012;3:353.
578 DOI: 10.3389/fphys.2012.00353.
579 52. Grundmann S, Piek JJ, Pasterkamp G, Hoefer IE. Arteriogenesis: basic mechanisms and
580 therapeutic stimulation. Eur J Clin Invest. 2007;37(10):755-66. DOI: 10.1111/j.1365-
581 2362.2007.01861.x.
582 53. Zhang J, Muri J, Fitzgerald G, Gorski T, Gianni-Barrera R, Masschelein E, D'Hulst G,
583 Gilardoni P, Turiel G, Fan Z, Wang T, Planque M, Carmeliet P, Pellerin L, Wolfrum C, Fendt SM,
584 Banfi A, Stockmann C, Soro-Arnaiz I, Kopf M, De Bock K. Endothelial Lactate Controls Muscle
585 Regeneration from Ischemia by Inducing M2-like Macrophage Polarization. Cell Metab.
586 2020;31(6):1136-53 e7. DOI: 10.1016/j.cmet.2020.05.004.
587 54. Naito Y, Takagi T, Higashimura Y. Heme oxygenase-1 and anti-inflammatory M2
588 macrophages. Arch Biochem Biophys. 2014;564:83-8. DOI: 10.1016/j.abb.2014.09.005.
589 55. Pan LL, Qin M, Liu XH, Zhu YZ. The Role of Hydrogen Sulfide on Cardiovascular
590 Homeostasis: An Overview with Update on Immunomodulation. Front Pharmacol.
591 2017;8:686. DOI: 10.3389/fphar.2017.00686.

592   56.   Wu J, Chen A, Zhou Y, Zheng S, Yang Y, An Y, Xu K, He H, Kang J, Luckanagul JA, Xian M,
593   Xiao J, Wang Q. Novel H2S-Releasing hydrogel for wound repair via in situ polarization of M2
594   macrophages. Biomaterials. 2019;222:119398. DOI: 10.1016/j.biomaterials.2019.119398.

595

596

Figure Legends.
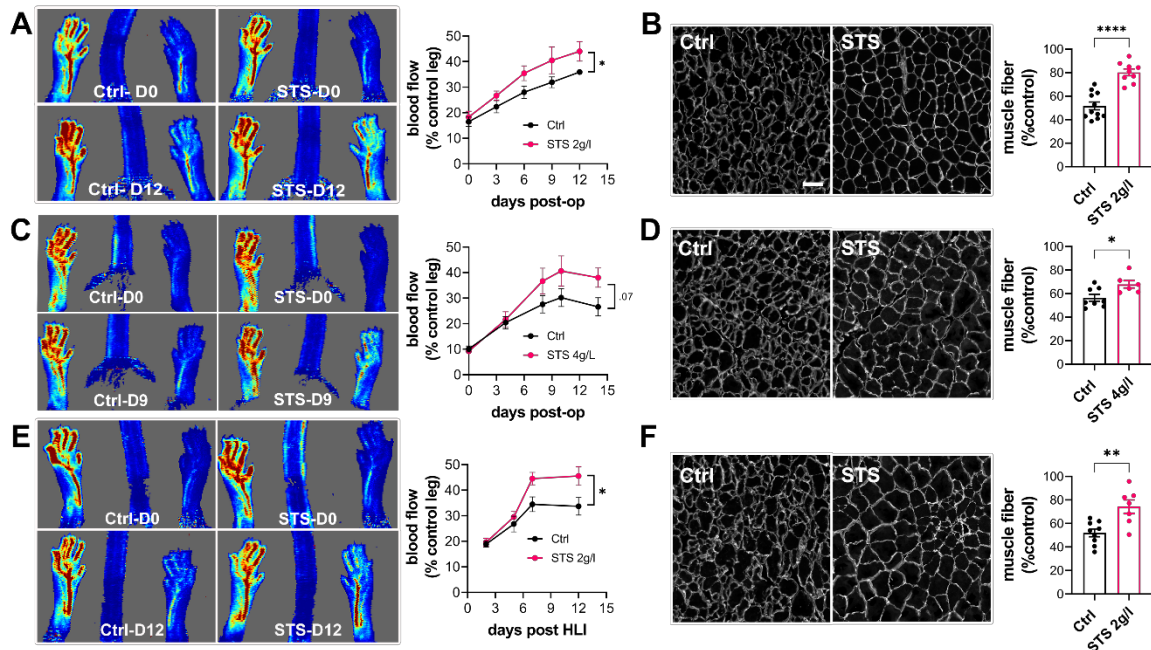
Figure 1 STS promotes revascularization and muscle recovery in a mouse model of hindlimb ischemia

Doppler imaging (**A, C, E**) and laminin immunostaining in the gastrocnemius muscle (**B, D, F**) of WT male mice submitted to HLI and treated or not (Ctrl) with 2g/L STS (**A-B**) or 4g/L STS (**C-D**), or LDLR-/- mice treated with 2g/L STS **(E-F).** (**A, C, E**) Data are mean ± SEM of 8 to 12 animals per group. *p<.05 as determined by repeated measures Mixed-effects model (REML). (**B, D, F**) Data are mean ± SEM of 6 to 12 animals per group. *p<.05, **p<.01; ****p<.0001 as determined by bilateral unpaired t-test. Scale bar 100 μm.
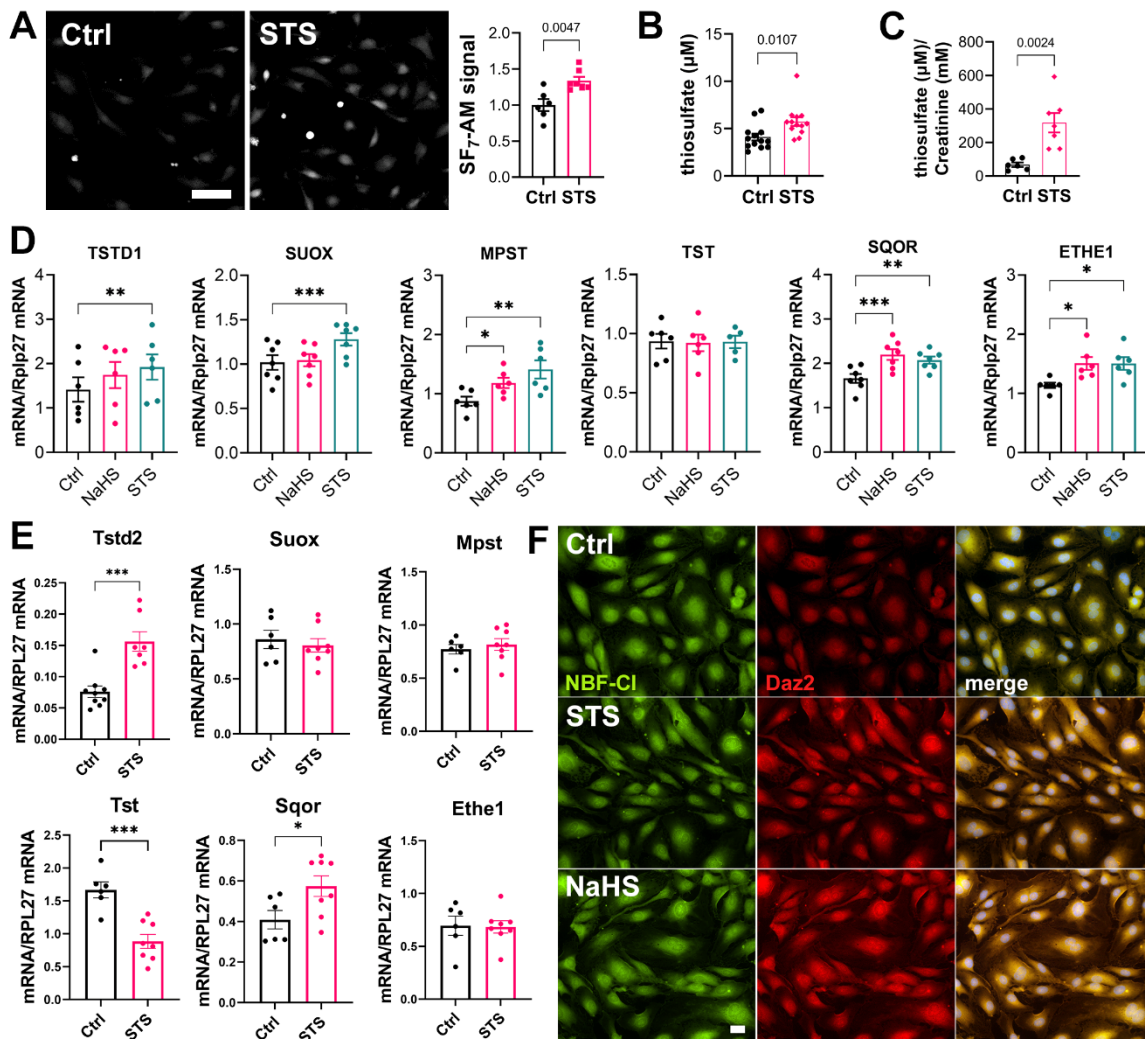
Figure 2. **STS leads to enzymatic production of H₂S and increases protein persulfidation.**

A) H$_2$S release measured by the SF$_7$-AM probe in HUVEC exposed for 90 min to STS. Data are mean ± SEM of 6 independent experiments. *p<.05 as determined by bilateral unpaired t-test. Scale bar 20 μm. **B)** Plasma levels of thiosulfate in mice treated or not (Ctrl) for 2 weeks with 4g/L STS. Data are mean ± SEM of 12 animals per group. p=.011 as determined by bilateral- unpaired t-test. **C)** Urine levels of thiosulfate, normalised to creatinine levels, in mice treated or not (Ctrl) for 2 weeks with 4g/L STS. Data are mean ± SEM of 6 or 7 animals per group. p=.0035 as determined by bilateral- unpaired t-test. **D)** mRNA expression in HUVEC exposed for 4h to NaHS (100μM) or STS (3mM). Data are mean ± SEM of 6 independent experiments. *p<.05, **p<.01; ***p<.001 as determined by repeated measures one-way ANOVA with Dunnett's post-hoc test. **E)** mRNA expression in gastrocnemius muscle of mice treated for 1 week with 4g/L STS. Data are mean ± SEM of 6 to 8 animals per group. *p<.05, **p<.01; ***p<.001 as determined by bilateral- unpaired t-test **F)** *In situ* labelling of intracellular protein persulfidation assessed by DAz-2:Biotin-Streptavidin-584 (red), normalized to NBF-adducts fluorescence (green), in HUVEC exposed for 4 hours to NaHS (100 μM) or STS (3mM).
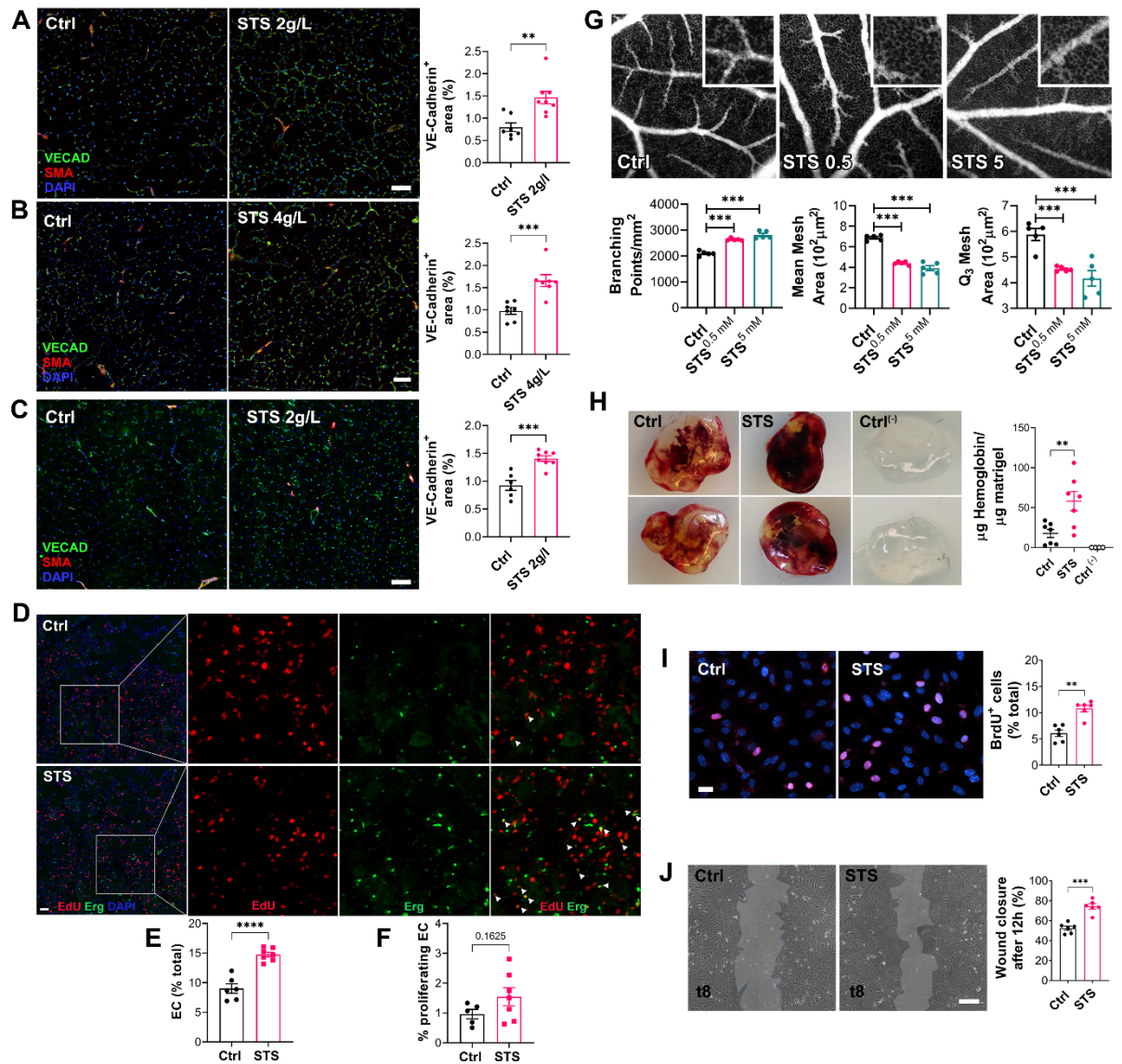
Figure 3 STS promotes angiogenesis in vivo in several models

A-C) VE-cadherin (VECAD; green), smooth muscle actin (SMA; red) and nuclei (DAPI; blue) immunostaining in gastrocnemius muscle from WT male mice submitted to HLI and treated or not (Ctrl) with 2g/L STS (**A**) or 4g/L STS (**B**), or LDLR-/- mice treated with 2g/L STS (**C**). Representative images and quantification of the VECAD staining in 6 to 9 animals per group. Data are mean ± SEM. **p<.01, ***p<.001 as determined by bilateral unpaired t-test. **D**) EdU (red), ERG (green) and nuclei (blue) immunostaining in ischemic muscle of WT mice treated with 2g/L STS 4 days after HLI. Scale bar represent 100 μm. Insets are 3-fold magnification of left images. **E**) Percentage of endothelial cells (ERG$^+$/total nuclei count). **F**) Percentage of proliferating endothelial cells (EdU$^+$/ERG$^+$). Data are mean ± SEM. *p<.05, ****p<.0001 as determined by bilateral unpaired t-test. **G**) Representative fluorescein-dextran fluorescence angiographies at EDD13, 48 h after topical treatment with 0.9% NaCl (Ctrl), or STS (0.5 or 5mM final). Representative images and quantification of the vascular network from 5 eggs per group. Data are mean ± SEM. ***p<.001 as determined by one-way ANOVA with Tukey's post-hoc test. **H**) Matrigel plugs supplemented or not (ctrl$^-$) with VEGF$_{135}$ +/- STS (15mM) 1 week post implantation. Representative plugs and haemoglobin content normalized to plug weight. Quantification of 4 to 8 animals per group. Data are mean ± SEM. **p<.01 as determined by one-way ANOVA with Tukey's post-hoc test. **I**) HUVEC proliferation assessed by BrdU incorporation and expressed as BrdU positive cells (pink) over DAPI positive nuclei. Data shown as mean ± SEM of 6 independent experiments. **p<.01 as determined by bilateral unpaired t-test. **J**) HUVEC migration was assessed by wound healing assay in presence of Mitomycin C and expressed as the

643   percentage of wound closure after 10 hours. Data shown as mean ± SEM of 6 independent experiments. **p<.01,

644   ***p<.001 as determined by bilateral unpaired t-test.
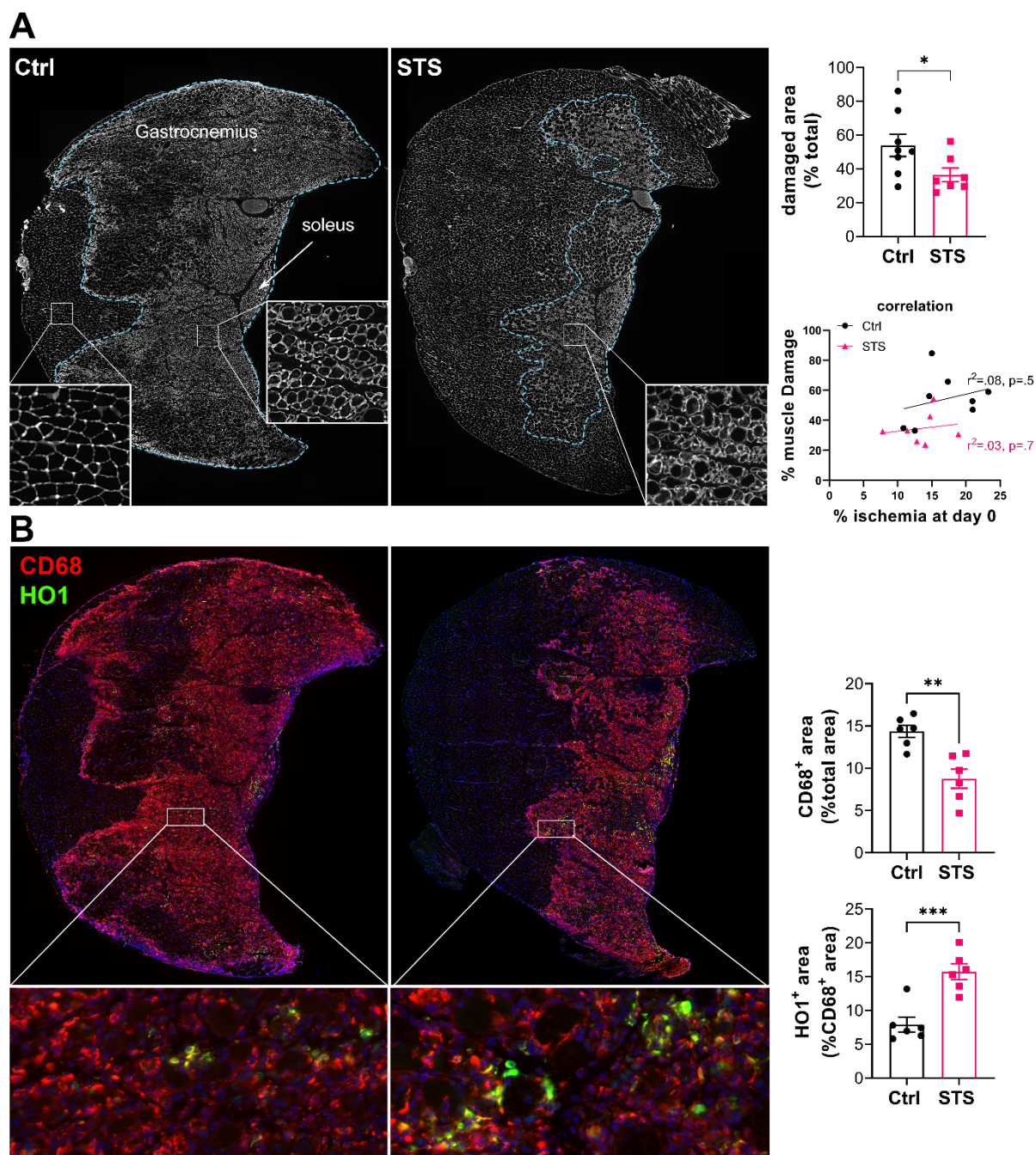
645

646   **Figure 4.**   **STS limits inflammation and muscle damage 4 days after ischemia**

647   **A)** Left panel: Representative images of gastrocnemius and soleus muscle of WT mice treated or not (Ctrl) with

648   4g/L STS, stained for laminin (white). Damaged area delimited by the blue dotted line. Right upper panel:

649   Quantification of the damaged area, expressed as a percentage of the total muscle area. Data are mean ± SEM.

650   *p<0.05 as determined by unpaired t-test. Right lower panel: correlation between muscle damage and ischemia

651   after the surgery. Data analysed by Pearson correlation. **B)** *Left panel:* Representative images of gastrocnemius

652   and soleus muscle of WT mice treated or not (Ctrl) with 2g/L STS, stained for CD68 (red) and HO1 (green). *Right*

653   *panel*: CD68 and HO1 positive area quantification. Data are mean ± SEM. **p<.01 ***p<.001 as determined by

654   bilateral unpaired t-test.
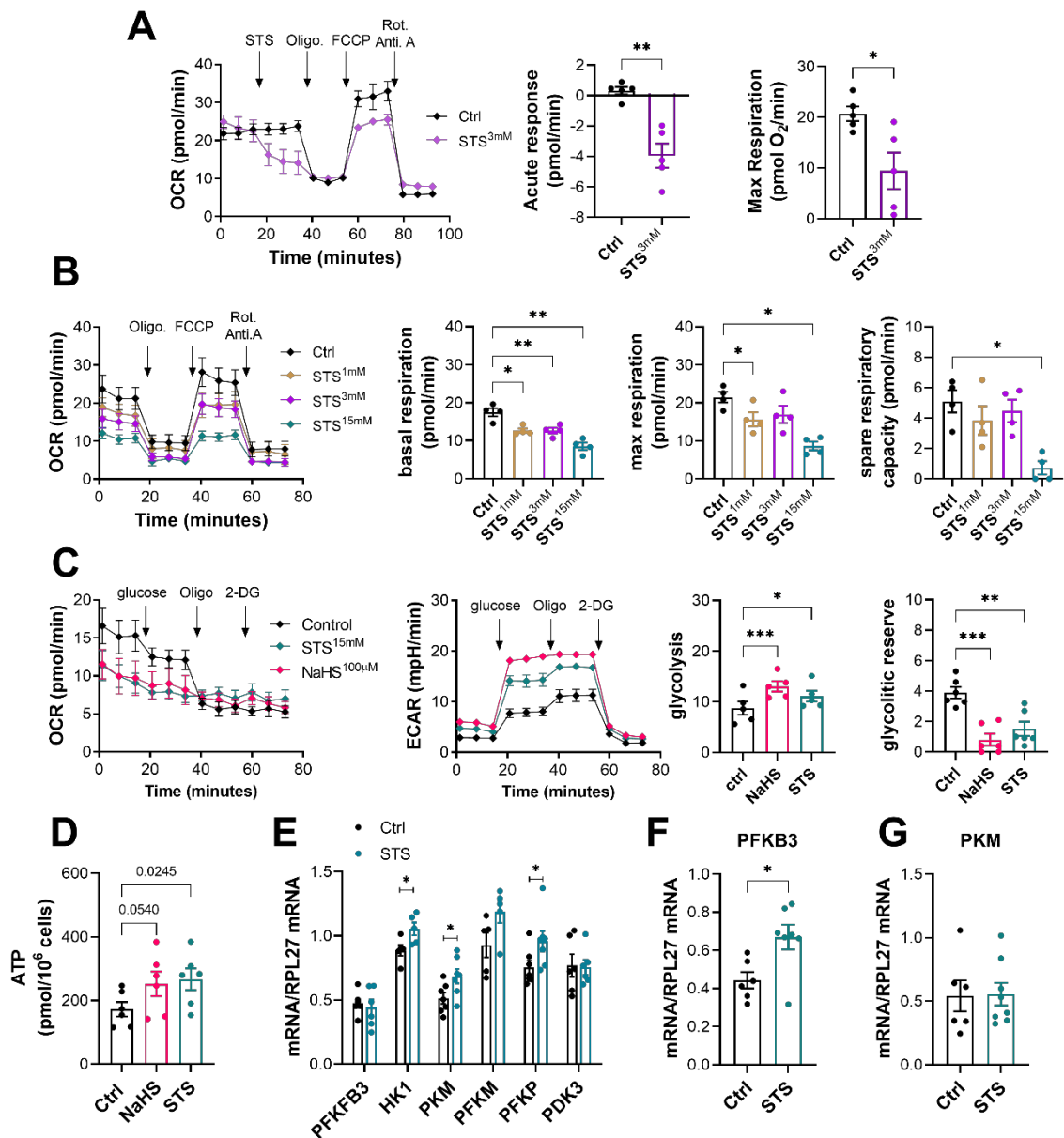
657 **Figure 5. STS inhibits mitochondrial respiration and increases glycolysis and ATP production in HUVECs.**

658 **A)** Acute effect of STS on respiration in a mitochondrial stress test assay using HUVEC. *Left panel:*
659 representative traces of oxygen consumption rate (OCR). *Right panels:* quantitative assessment of decreased
660 OCR in response to STS injection and maximal respiration upon FCCP injection. Data are mean ±SEM of 5
661 independent experiments. *p<.05, **p<.01 as determined by bilateral unpaired t-test. **B**) Mitochondrial stress
662 test in HUVEC pre-treated for 4h with increasing concentration of STS, as indicated. Data are mean±SEM of 54
663 independent experiments. *p<.05, **p<.01 as determined by repeated measures mixed-effects model (REML)
664 followed by Dunnett's multiple comparisons tests. **C**) Glycolysis stress test in HUVECs pre-treated for 4h with
665 3mM STS or 100µM NaHS. Glycolysis is measured by extracellular acidification rate (ECAR). Data expressed as
666 mean±SEM of 5 independent experiments. *p<.05, **p<.01, ***p<.001 as determined by repeated measures
667 mixed-effects model (REML) followed by Dunnett's multiple comparisons tests. **D**) ATP production in HUVEC
668 treated for 24h with 100µM NaHS or 3mM STS. Statistics are p-values determined by bilateral unpaired t-test.
669 **E**) Normalized mRNA levels of key glycolysis genes in HUVEC pre-treated for 4h with 15mM STS. Data are

mean±SEM of 7 independent experiments. *p<.05 as determined by bilateral unpaired t-test. **F-G**) PFKFB3 (**F**) and PKM (**G**) mRNA levels in the gastrocnemius muscles of mice treated or not with 4g/L STS for 1 week. Data are mean±SEM of 7 animals per group. *p<.05 as determined by bilateral unpaired t-test.
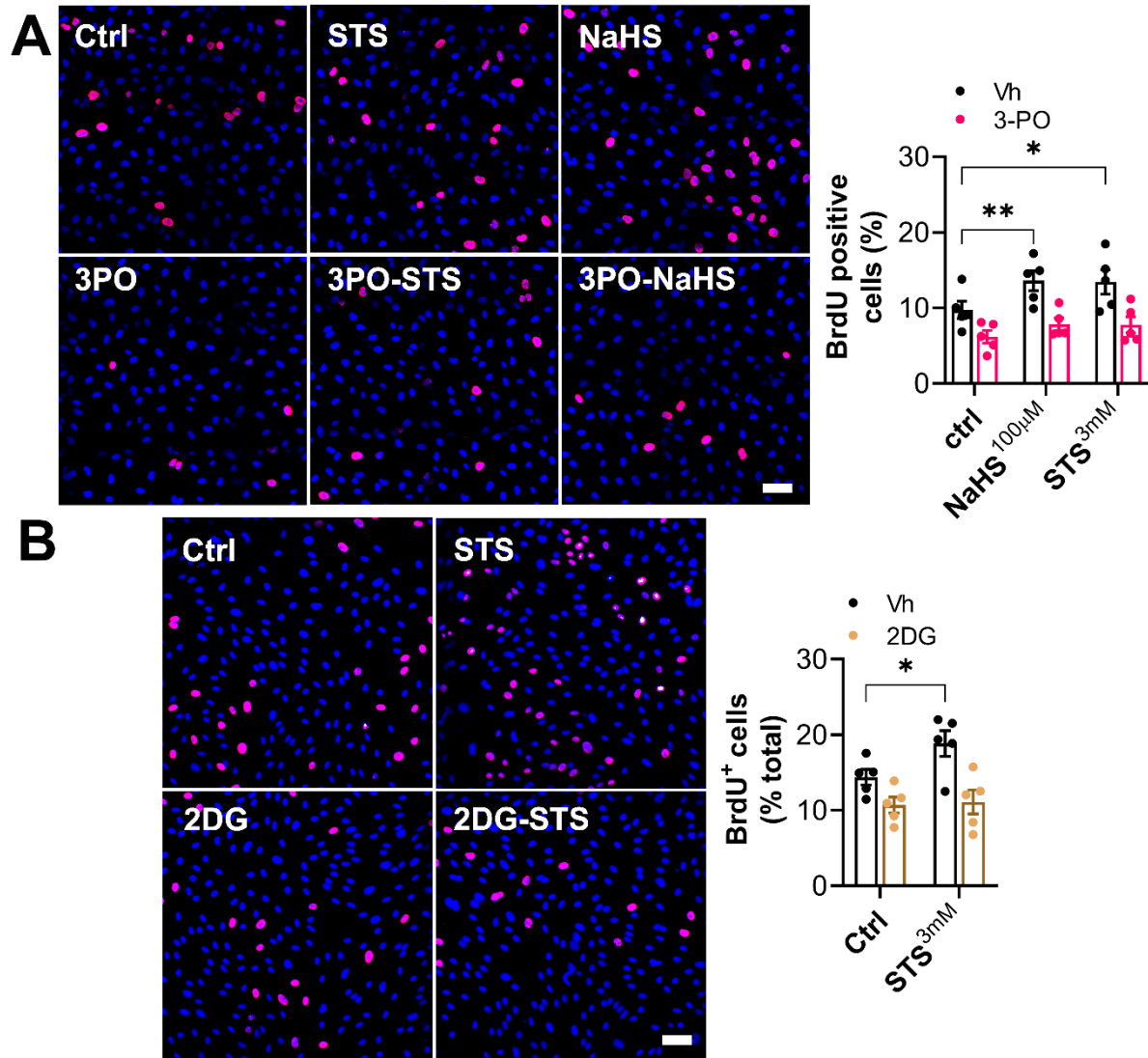
Figure 6. STS-induced HUVEC proliferation requires glycolysis

A-B) HUVEC proliferation (BrdU incorporation) in cells treated for 8h with 100µM NaHS, 3mM STS +/- 15µM PFKFB3 inhibitor (3-PO) or 6mM 2 deoxy-glucose (2DG), or their respective vehicle (Vh). *Left Panels:* representative images. *Right panels:* Data are mean ± SEM of ratio of BrdU positive cells (pink) over DAPI positive nuclei (blue) in 5 independent experiments. *p<0.05 as determined by repeated measures two-way ANOVA with Dunnett's post-hoc test.